Electronic Supplementary Information

Simultaneous non-covalent bi-functionalization of 1T-MoS_2 ruled by electrostatic interactions: towards multi-responsive materials

Daniel Iglesias,[a] Stefano Ippolito,[a] Artur Ciesielski*[a], Paolo Samorì*[a]

a. Université de Strasbourg, CNRS, ISIS, 8 allée Gaspard Monge, 67000 Strasbourg, France. E-mail : ciesielski@unistra.fr , samori@unistra.fr

Table of contents

1. Experimental part

1.1 Materials: Bulk MoS_2 (< 2 μm, 98%) and the rest of chemicals and solvents were purchased from Sigma-Aldrich and used without further purification. Ferroin was synthesized by mixing 1 equivalent of $FeSO_4$ and 3 equivalents of *o*-phenantroline in water.

1.2 Equipment:

UV-Vis spectra were recorded on a JASCO V-670 spectrophotometer in 1 cm path quartz cuvettes. ce-MoS_2 solutions were diluted 30 times before analysis. For the kinetics experiments, a fixed wavelength was measured every 20 s during 30 min. The cuvette was kept at 25 °C and stirred (500 rpm) using a Peltier Cell Changer.

Thermogravimetric analysis was performed under nitrogen, from 25 to 800 °C with a ramp of 10 °C on a Mettler Toledo TGA/SDTA851e. ce-MoS_2 solutions were freeze-dried before analysis.

Zeta potential of ce-MoS_2 solutions was recorded on Delsa Nano C Particle Analyzer (Beckman Coulter, Brea, CA, USA).

Raman analysis was done in a Renishaw InVia Reflex Reflex instrument equipped with a high-resolution grating (2400 grooves cm^{-1}), a confocal microscope and a 2D-CCD camera. All samples were focused with a ×100 lens and were excited with a green laser (532 nm). Three different analysis are reported. The dyes and the corresponding hybrids were irradiated at different intensities (0.02-2.86 mW) for 10 s. To characterize the presence of 1T phase, all MoS_2 samples were irradiated at 0.03 mW for 16 s (4 accumulations lasting 4 s each). More than 20 data points were average out to ensure the homogeneity of the samples. The Raman point-mapping method with the ×100 microscope provided a spectral resolution of ~0.46 μm^2. The samples were irradiated at 0.03 mW for 4 s (2 accumulatios of 2 s each).

X-ray photoelectron spectroscopy (XPS) data was acquired on a Thermo Scientific K-Alpha X-ray photoelectron spectrometer equipped with an aluminum X-ray source (energy 1486.6 eV) at a base pressure of 10^{-8}–10^{-9} mbar. The X-ray beam spot size was ~400 μm. Survey spectra were recorded as an average of 10 scans with a pass energy of 200.00 eV and a step size of 1 eV; high-

resolution spectra were an average of 10 scans with a pass energy of 50.00 eV and a step size of 0.1 eV. The materials were all analyzed in the form of dry films.

Atomic force microscopy (AFM) characterization was performed with a Bruker Dimension Icon microscope under ambient conditions. As-prepared ce-MoS_2 solutions were diluted 10 times and spin coated (3000 rpm, 45 s, 10 times) on Si wafer. Bruker TESPA-V2 tips (spring constant k = 42 N/m) were used to obtained images resolved by 512×512 or 1024×1024 pixels in tapping mode.

Scanning electron microscopy images were collected under vacuum in a Quanta FEG 250 (FEI) system operating at max. 30 kV equipped for energy dispersive X-Ray analysis.

Electrical resistance of D@ce-MoS_2 films was measured using four-point probe analyzer (RM-3000, Jandel). The current was maintained between 0.1 and 0.5 μA to keep a voltage between 0.4-0.5 mV.

Bending cycles were done using a digital force gauge (Mark-10, M7-025E, ~1.0 N) with motorized test stand (Mark-10, ESM-303E). Ten rounds of 1000 bending cycles were performed. The electrical conductivity of the substrate was checked after every round.

2. Chemical exfoliation of MoS_2

The reaction was carried out in a Schlenk tube under dry and inert atmosphere. *n*-BuLi (1.6 M, 2.5 mL) was added to a mixture of MoS_2 (250 mg) and dry hexane (2.5 mL). The reaction was stirred at 55 °C for 24 h. After that, it was diluted with hexane (6 mL) and quenched with H_2O (2 mL). The crude was diluted with H_2O (50 mL) and washed with hexane (4 x 50 mL). The aqueous phase was made up to 250 mL and sonicated for 1 h at room temperature. The dispersion was centrifuged (750 rpm, 30 min), dialyzed against water (24 h) and flushed with nitrogen (1 h) affording ce-MoS_2 dispersions (~0.8 mg/mL).

3. Characterization of ce-MoS_2

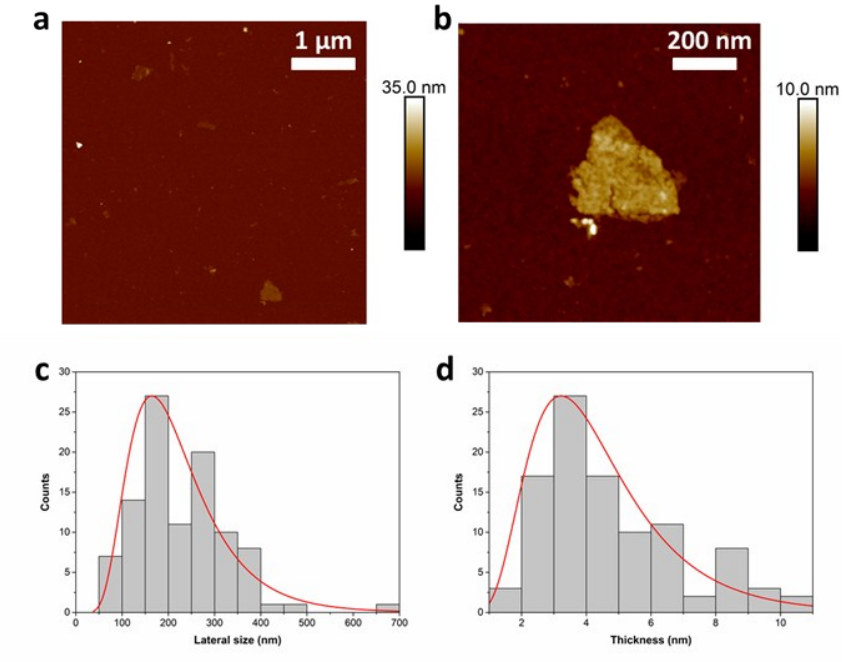

Figure S 1. (a, b) Topographical AFM image of ce-MoS_2. Statistical analysis showing (c) the lateral size, and (d) the thickness of the exfoliated layers.

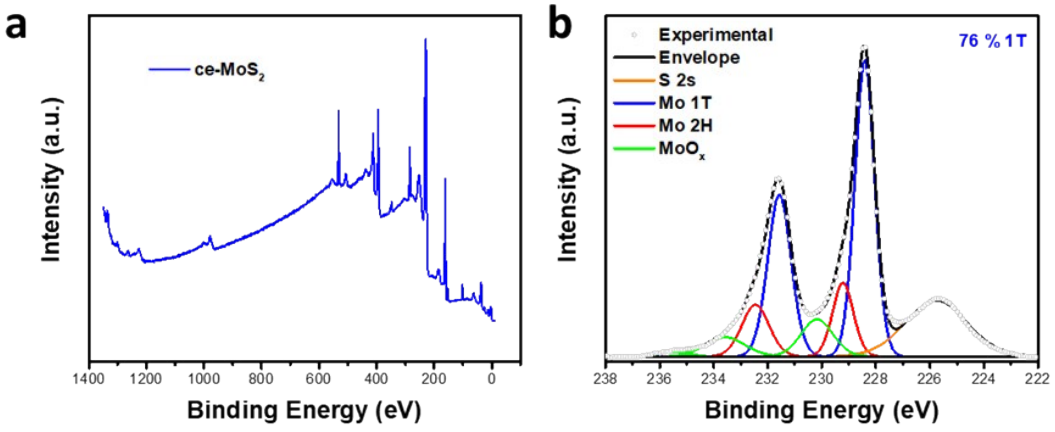

Figure S 2. XPS spectrum of ce-MoS_2: (a) survey, (b) high-resolution Mo 3d deconvoluted spectrum showing the dominant presence of 1T phase.

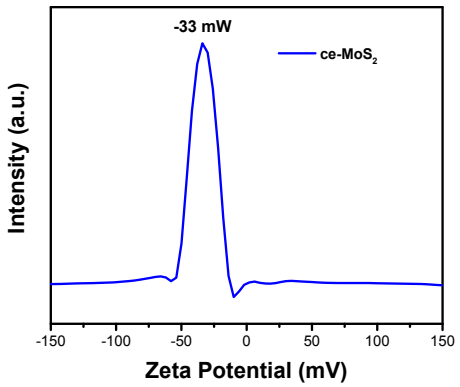

Figure S 3. Zeta potential measurement of ce-MoS_2.

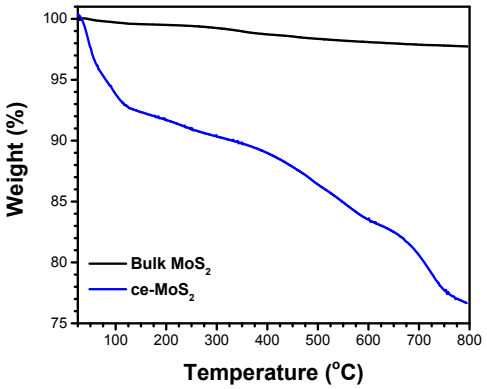

Figure S 4. Thermogravimetric analysis of bulk MoS_2 and ce-MoS_2. ce-MoS_2 was freeze-dried and the solid sample was analyzed by thermogravimetric analysis. The thermograms evidence a dramatic decrease of thermal resistance after exfoliation. This effect is attributed to introduction of defects during the process, and it agrees with other literature reports.[1]

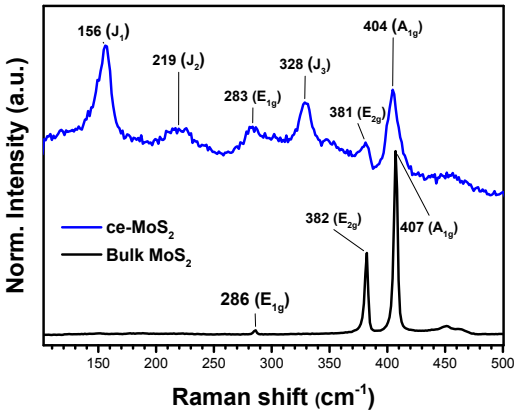

Figure S 5. Raman spectra of bulk MoS_2 and ce-MoS_2. The Raman fingerprint of bulk MoS_2 is characterized by the E^1_{2g} and A_{1g} peaks at ~382 and ~407 cm^{-1}, respectively. The dominant presence of 1T ce-MoS_2 is confirmed by the peaks at 156 cm^{-1} (J_1), 219 cm^{-1} (J_2) and 328 (J_3). E^1_{2g} and A_{1g} peaks are broaden and less intense.

Calculation of the 1T % by UV-Vis

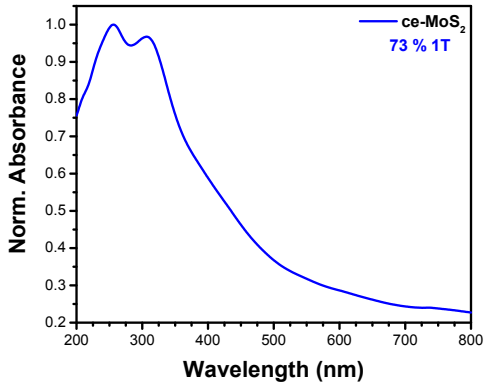

Figure S 6. UV-Vis spectrum of ce-MoS_2.

The estimation of 1T % exploiting the absorbance spectrum was done according to Equation S1. A_{410} and A_{350} are the absorbance at 410 and 350 nm, respectively.[1] The calculated value fits very well with the values obtained from XPS analysis (73 and 76 % 1T, respectively).

$$\frac{2H}{2H+1T} = 1.29 - (2.562 \times 0.287^{\frac{A_{410}}{A_{350}}}) \quad \text{Eq. S1.}$$

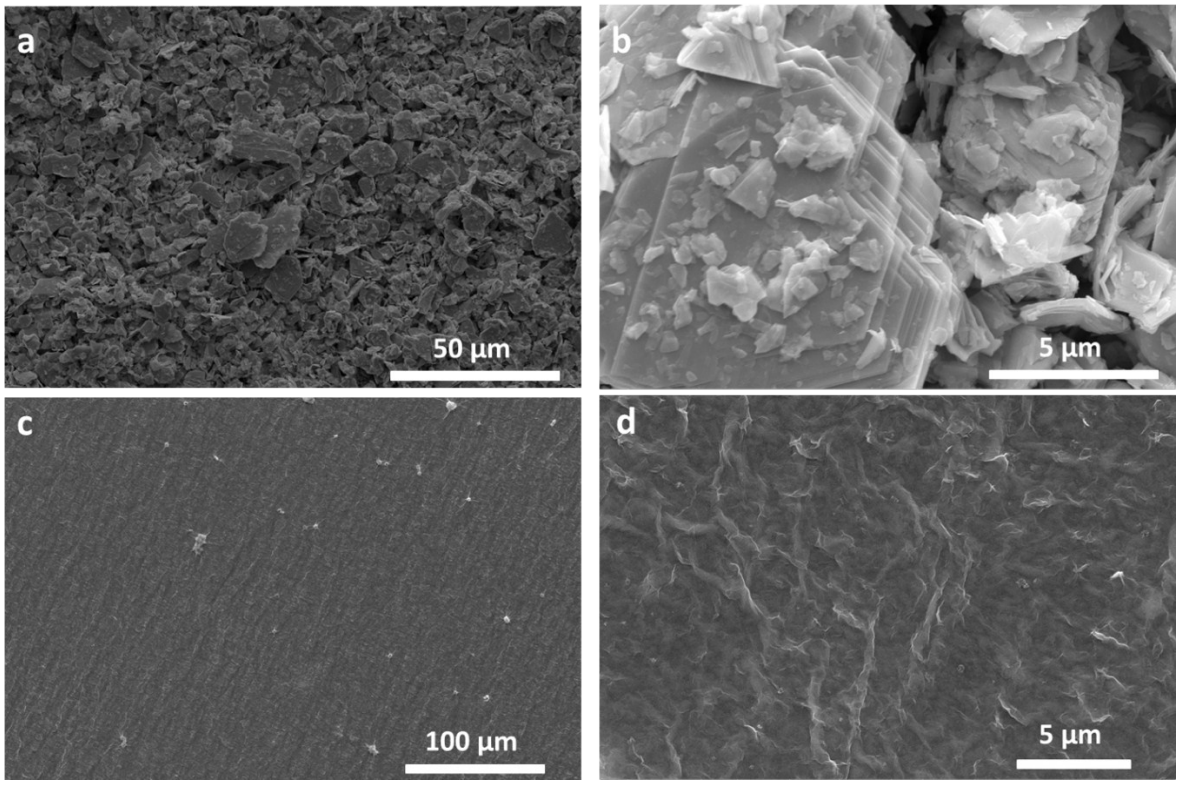

Figure S 7. SEM images of (a, b) bulk MoS_2, and (c, d) ce-MoS_2. Bulk MoS_2 is composed of few-micrometer size layered particles that form very rough films. On the other hand, ce-MoS_2 nanosheets form films with reduced roughness, as expected for exfoliated 2D materials.

4. Supramolecular functionalization of ce-MoS_2.

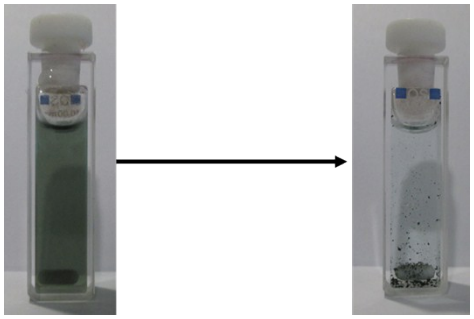

Figure S 8. Images of a dispersion of a fresh ce-MoS_2 and MB in water (left) and after 15 min stirring (right).

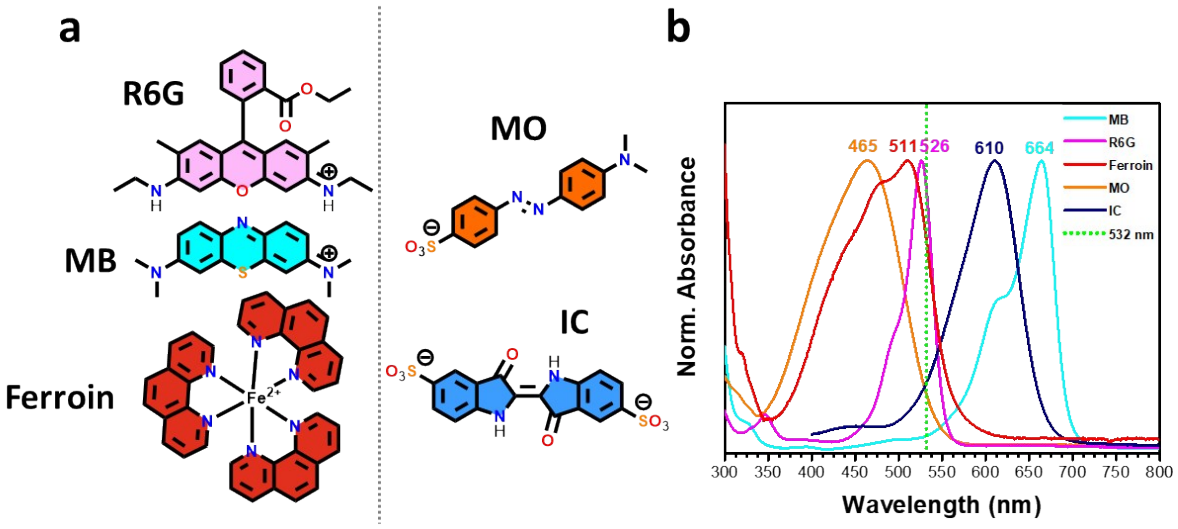

Figure S 9. (a) Library of charged compounds used in this study. (b) UV-Vis spectra for the different dyes. The number on top of the curves correspond to the maximum of absorbance. The dotted line in the spectrum represents the position of the green laser used for the Raman analysis.

4.1 Effect of dye: ce-MoS_2 ratio

The experiment was done in 4 mL-glass vials. Ten different samples for every dye were prepared. The composition of the different samples is detailed in Table S1. The prepared solutions were stirred in a laboratory rotator for 1 h to ensure the complete interaction. Finally, the UV-Vis spectrum of all solutions was collected and the molar absorptivity of the dyes was used to calculate its concentration ($\varepsilon_{MB@664} = 95000\ M^{-1}\ cm^{-1}$, $\varepsilon_{R6G@527} = 116000\ M^{-1}\ cm^{-1}$, $\varepsilon_{Ferroin@511} = 11000\ M^{-1}\ cm^{-1}$, $\varepsilon_{MO@464} = 25100\ M^{-1}\ cm^{-1}$, $\varepsilon_{IC@527} = 11700\ M^{-1}\ cm^{-1}$).

Note: the scattering was corrected to calculate the dye concentration.

Table S 1. Composition of all solutions in the designed experiment.

Sample	Vol. dye (mL)	Vol. ce-MoS_2 (mL)
1	1.5	0
2	1.5	0.1
3	1.5	0.2
4	1.5	0.3
5	1.5	0.4
6	1.5	0.5
7	1.5	0.6
8	1.5	0.75
9	1.5	1.0
10	1.5	1.5

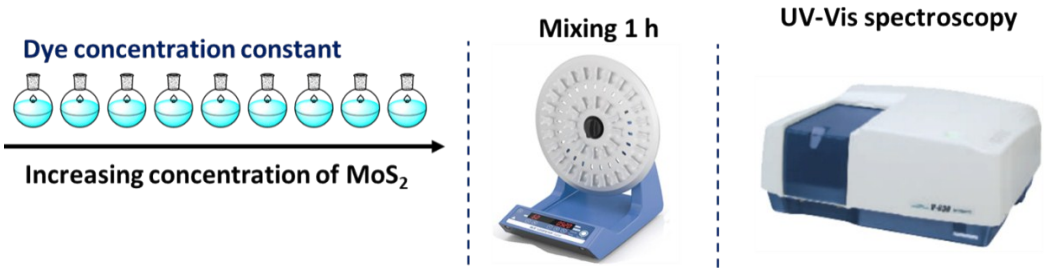

Figure S 10. Schematic representation of the different steps of the experiment.

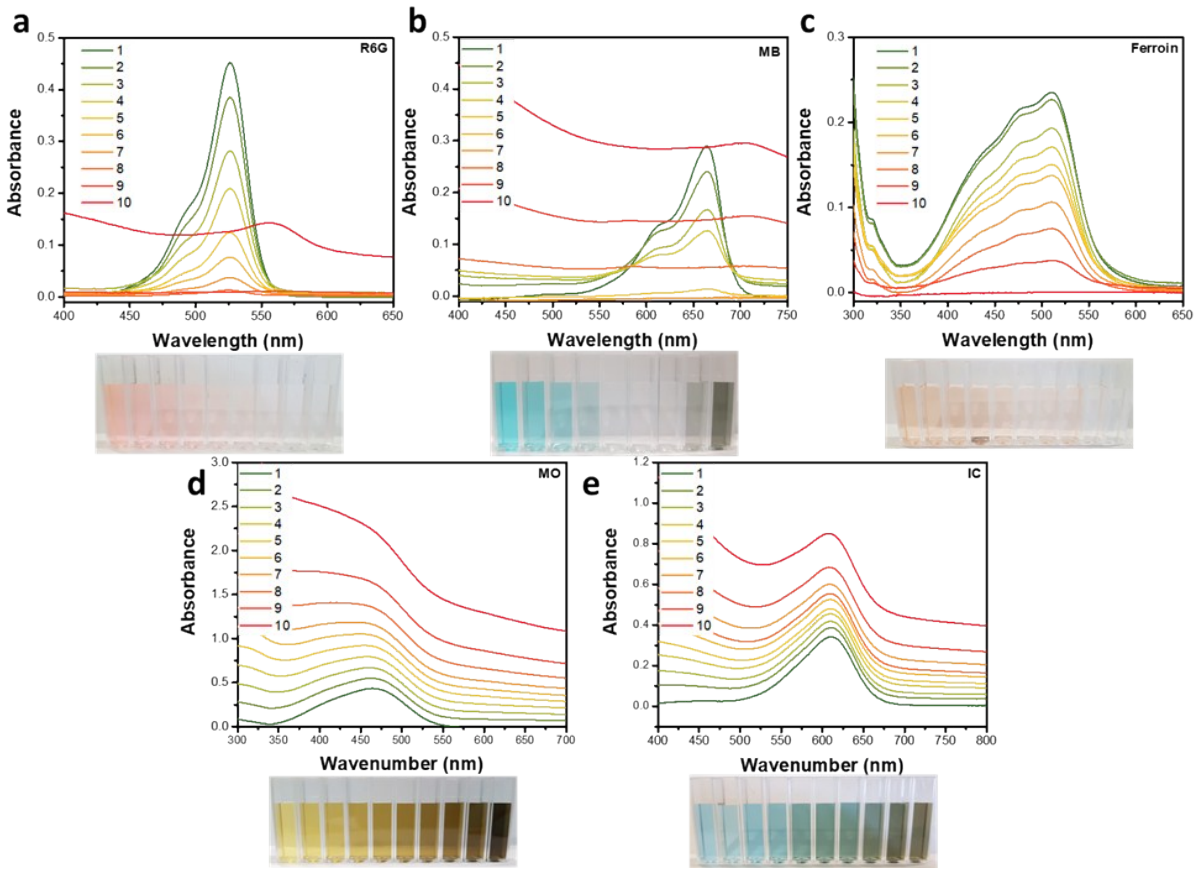

Figure S 11. Raw UV-Vis data for the interaction of ce-MoS_2 with (a) R6G, (b) MB, (c) ferroin, (d) MO, and (e) IC. The image under every panel shows the analyzed solutions. The different behavior of positively and negatively charged dyes is clearly observed.

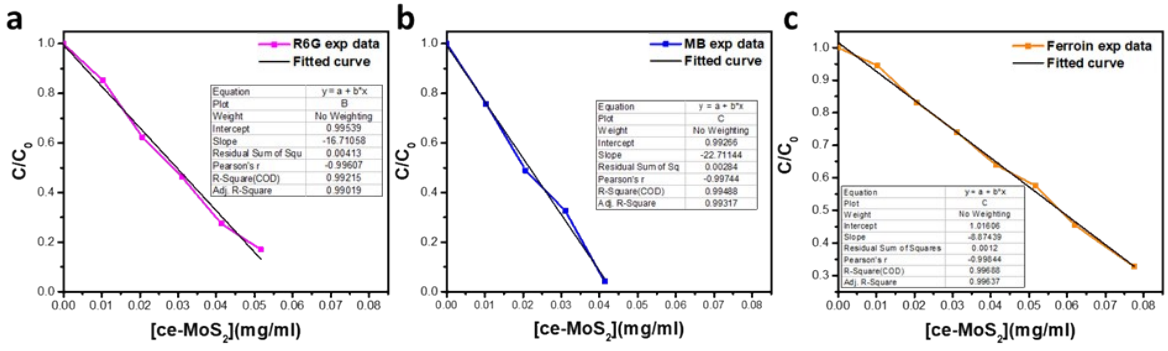

Figure S 12. Experimental data and fitting curves for the (a) R6G, (b) MB, and (c) ferroin. The normalized concentration of the dyes vs the ce-MoS_2 concentration is depicted.

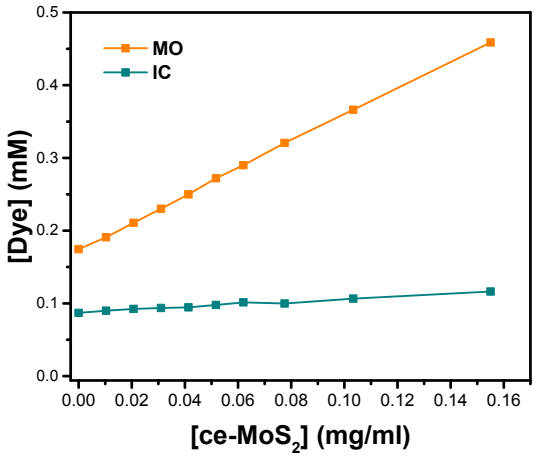

Figure S 13. Concentration of the negatively charged dyes at the different ce-MoS_2 concentrations. Note: Light scattering hinders the precise determination of the concentration, especially for MO with a maximum of absorbance at 465 nm.

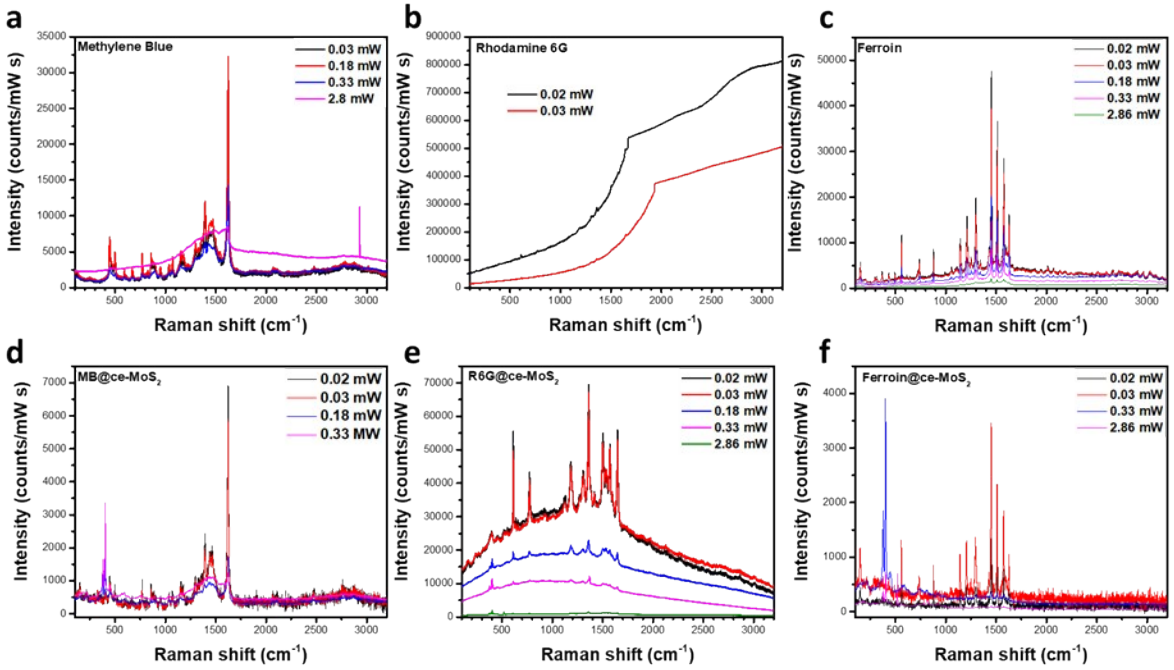

Figure S 14. Raman spectra of (a) MB, (b) R6G, and (c) ferroin and the corresponding hybrids (d) MB@ce-MoS_2, (e) R6G@ce-MoS_2, and (f) ferroin@ce-MoS_2 at different laser intensities (0.02-2.86 mW). The transformation from 1T to 2H phase at moderate laser intensities is observed (*i.e.* 0.33 mW). Besides, the data confirm the integrity of the dyes, in all cases, after the supramolecular functionalization. The analyses were carried out in Resonance Raman conditions, in particular, for R6G and ferroin. This, together with the solid nature of the functionalized ce-MoS_2, makes any analysis of SERS effect very challenging.

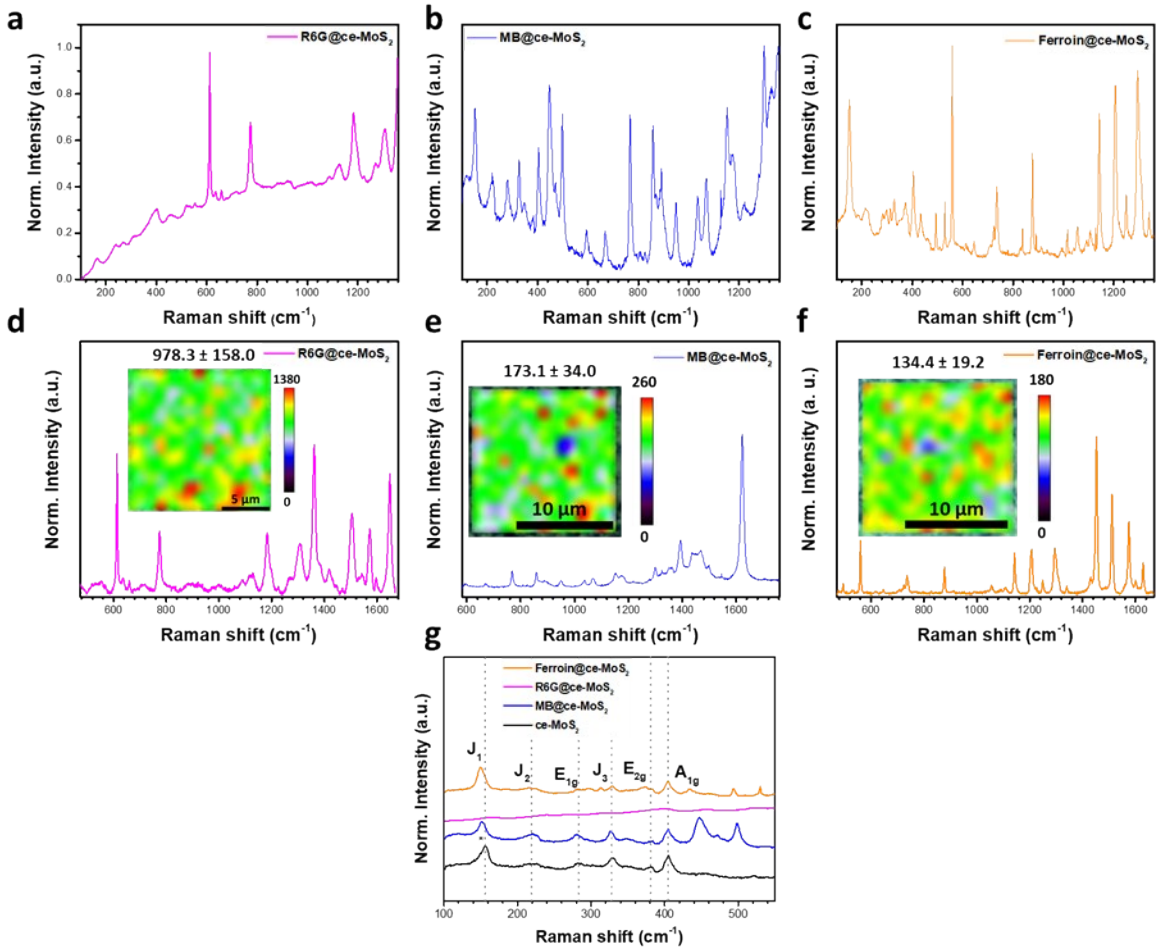

Figure S 15. Raman characterization of dye@ce-MoS_2 hybrids focusing on the small wavenumber to confirm the presence of 1T phase (a) R6G@ce-MoS_2, (b) MB@ce-MoS_2, and (c) ferroin@ce-MoS_2. The displayed ones aer the average Raman spectra out of 225 data points, the inset corresponds to the mapping of the peak at 612, 1623 and 1452 cm^{-1} for (d) R6G@ce-MoS_2, (f) MB@ce-MoS_2, and (f) ferroin@ce-MoS_2, respectively. The average intensity is displayed above the mapping. Overlapped spectra of ce-MoS_2 MB@ce-MoS_2, R6G@ce-MoS_2, and ferroin@ce-MoS_2 (g) showing the presence of J_1, J_2 and J_3 Raman modes in all samples. The J_1 peak is red-shifted in MB@ce-MoS_2 and ferroin@ce-MoS_2, while the E_{2g} and A_{1g} showed no shifting. The high background signal of R6G@ce-MoS_2 does not allow the evaluation of the shifting.

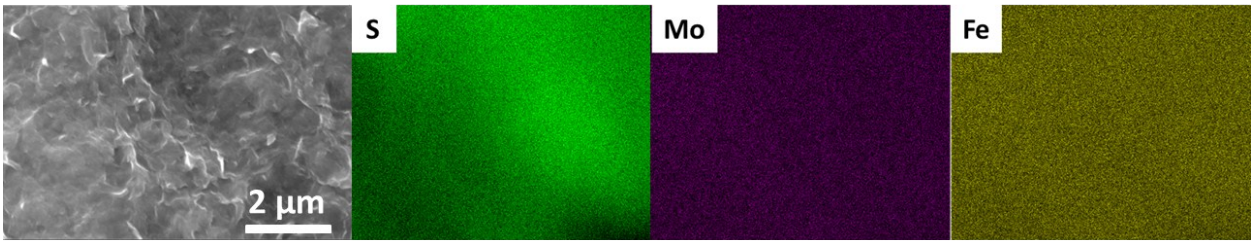

Figure S 16 SEM-EDX imaging of ferroin@ce-MoS_2.

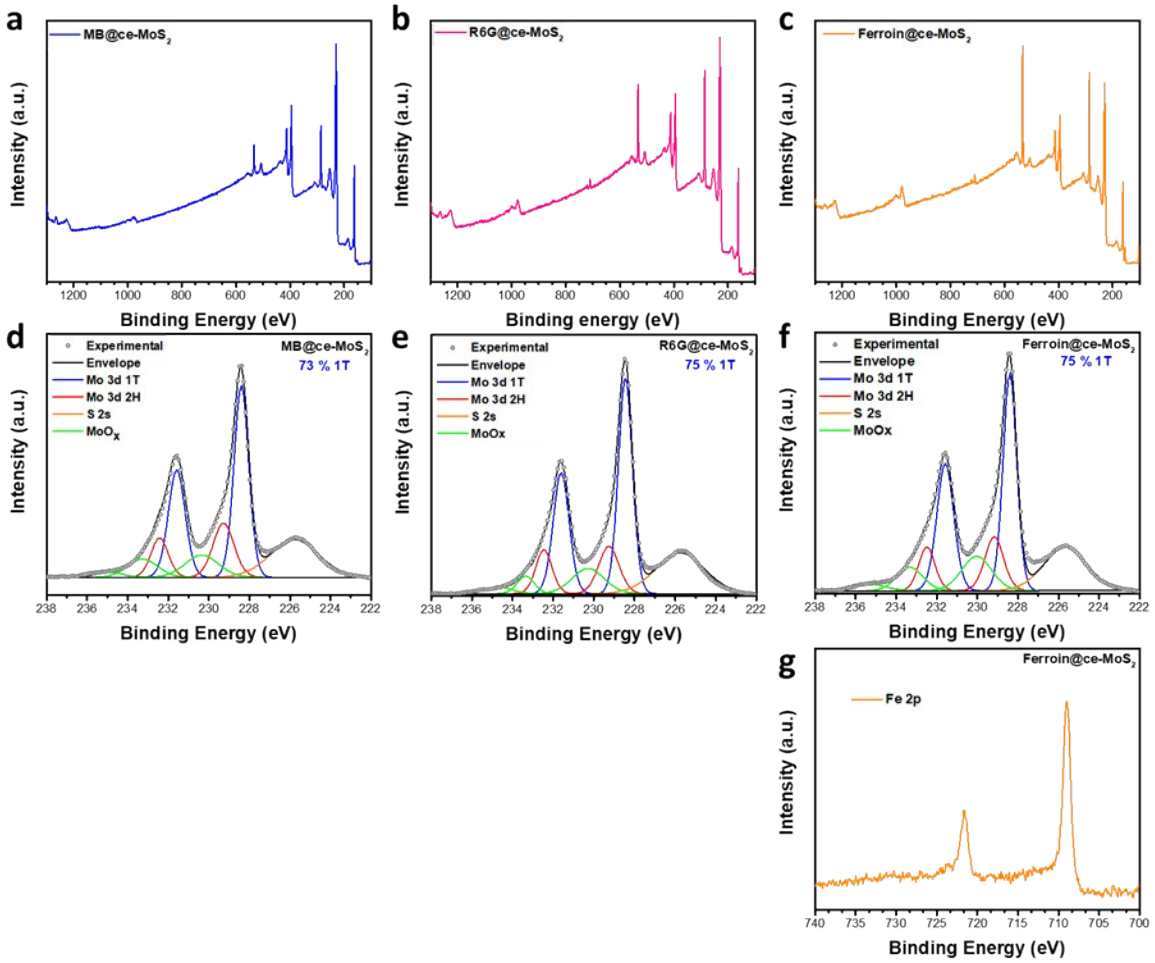

Figure S 17. XPS characterization including the survey and the high-resolution Mo 3d spectra for (a,d) MB@ce-MoS_2, (b,e) R6G@ce-MoS_2, and (c,f) ferroin@ce-MoS_2. (g) High-resolution Fe 2p for ferroin@ce-MoS_2.

4.2 Calculation of the degree of functionalization

The spectroscopic characterization of the process for the different dyes is very useful to calculate the degree of functionalization. An example of how this parameter is calculated is illustrated below for MB@ce-MoS_2.

Initial concentration of MB: 0.031 mM or 0.0086 mg mL^{-1}

Initial concentration of ce-MoS_2: 0.31 mg mL^{-1}

- 1.5 mL of MB were fully adsorbed by 0.6 mL of ce-MoS_2.
- Calculate the mass of the different components

$$1.5\ ml \times 0.0086 \frac{mg}{ml} = 0.0131 mg\ of\ MB^{+}$$

$$0.6\ ml \times 0.31 \frac{mg}{ml} = 0.0186\ mg\ of\ ceMoS_2$$

- Therefore, the total mass of the solid correspond to:
  $0.0131\ mg + 0.0186\ mg = 0.0318\ mg\ of\ MB@ceMoS_2$
  and the percentage of MB is:
  $$\frac{mass_{MB}}{mass_{MB@ceMoS_2}} \times\ 100 = \frac{0.0131}{0.318} \times 100 = 41\ \%$$

Table S 2. Degree of functionalization of dye@ce-MoS_2 hybrids.

Ref.	% dye in the hybrid
MB@ce-MoS_2	41
R6G@ce-MoS_2	45
Ferroin@ce-MoS_2	28
D@ce-MoS_2	10 for MB and 16 for ferroin

4.3 Synthesis of dye@ce-MoS_2 hybrids at large scale

The data extracted from Figure S11 has been extrapolated to prepare the hybrids at larger scale. 0.6 mL of ce-MoS_2 are required to fully adsorbed 1.5 mL of MB stock solution. Therefore, ce-MoS_2 (50 mL) and MB (125 mL) were stirred for 15 min at room temperature. The solution was

filtrated through a Millipore membrane (JHWP 0.45 µm) and the product was completely dried under vacuum. The same strategy was used for all hybrids.

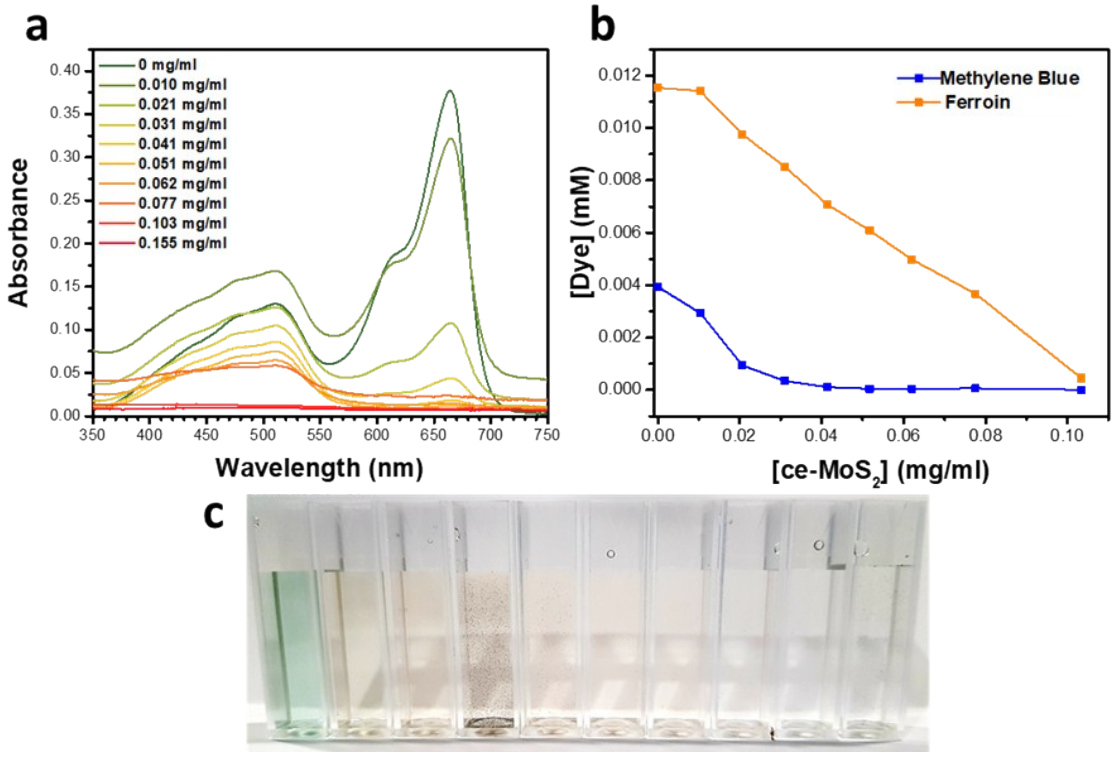

Figure S 18. Study of the simultaneous adsorption of MB and Ferroin on ce-MoS_2: (a) UV-Vis spectra, (b) concentration of the dyes vs concentration of ce-MoS_2, and (c) picture of the analyzed solutions.

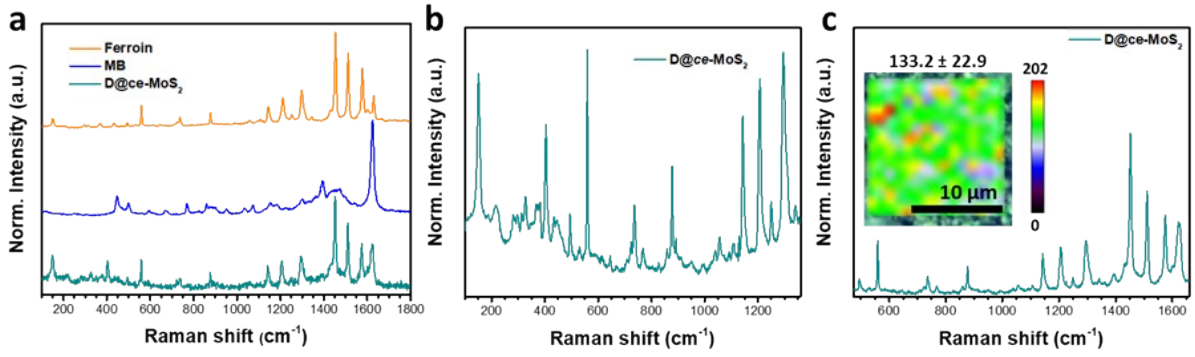

Figure S 19. (a) Raman characterization of D@ce-MoS_2: spectra of MB, ferroin and D@ce-MoS_2 showing the presence of both compounds in the hybrid. (b) Raman spectrum showing J_1 peak attributed to 1T ce-MoS_2 (b). (c) Raman spectrum out of 225 data points, the inset corresponds to the mapping of the peak at 1453 cm^{-1}. The average intensity is displayed above the mapping.

4.4 Kinetics and reversibility

In a typical kinetic study, a quartz cuvette was charged with aqueous MB and Ferroin at similar concentrations. The solution was stirred (500 rpm) at 25 °C. The absorbance of the dyes was measured every 20 s. After 5 min, ce-MoS_2 (50 µL) was added. The absorbance was performed for 25 min. A plateau was reached around 11 min after the ce-MoS_2 addition. This solution was used for the reversibility tests.

The aggregated D@ce-MoS_2 was bath sonicated for 1 min. After that, a full spectrum of the re-dispersed hybrid was recorded, before stirring the cuvette for 11 min, and another full spectrum was collected. The corresponding spectra are plotted in Figure S20.

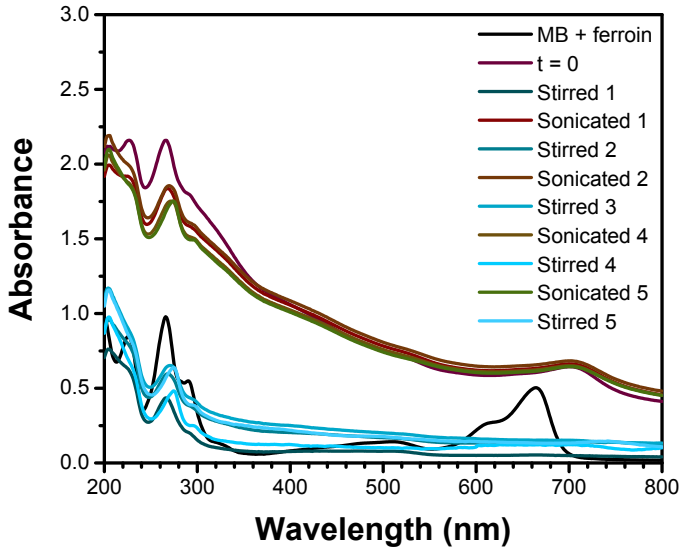

Figure S 20. Reversibility of the process. Absorbance spectra during the five stirring/sonication cycles. Only subtle variations were observed between cycles, which were attributed to experimental error and scattering effects.

5. Dry-transfer of D@ce-MoS_2 films.

A fresh dispersion of the as-prepared D@ce-MoS_2 was filtered through a Millipore membrane filter (JHWP 0.45 µm). The films were pressed against the target substrate (*e.g.* SiO_2/Si, glass or PET) for 2 h. After that, the Millipore membrane was carefully peeled off obtaining homogeneous films.

Note: Complete drying of the films makes the transfer more challenging.

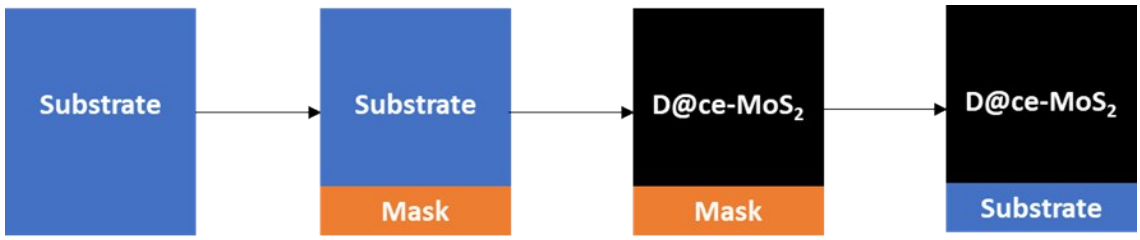

Figure S 21. Graphic representation of the dry-transfer procedure.

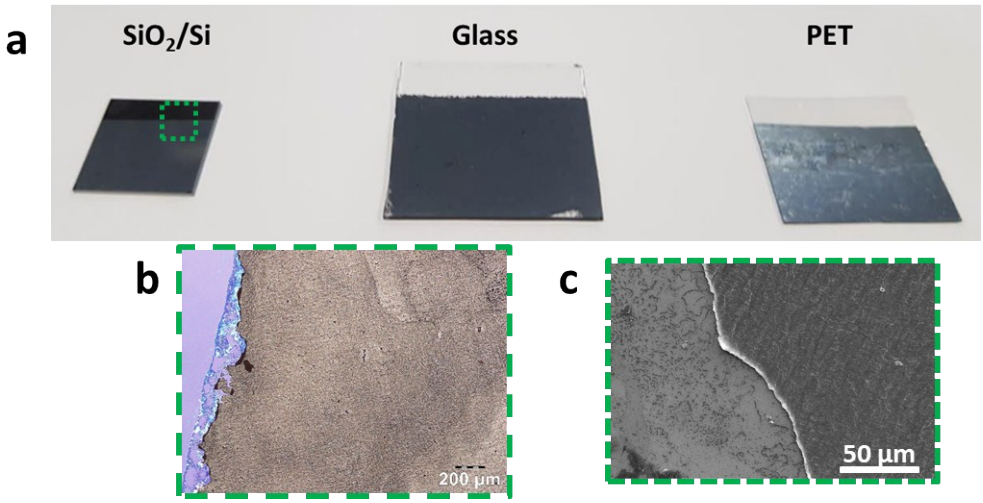

Figure S 22.(a) Photographs of D@ce-MoS_2 deposited on SiO_2/Si, glass and PET. (b) Optical microscopy, and (c) SEM images of the area highlighted in green.

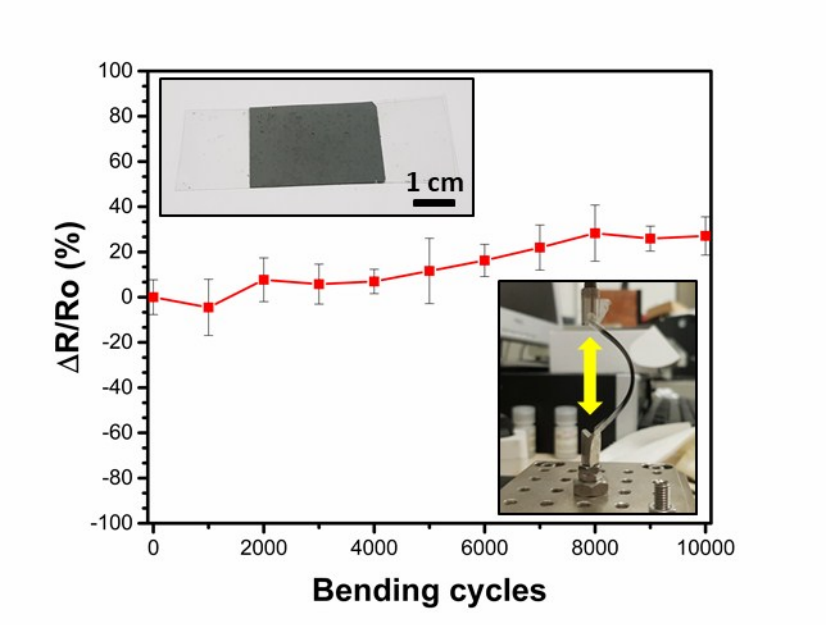

Figure S 23. Normalized resistance changes during the bending cycles. The insets show the tested substrate as prepared (top left) and in the bending state (bottom right).

6. References

1 K. C. Knirsch, N. C. Berner, H. C. Nerl, C. S. Cucinotta, Z. Gholamvand, N. Mcevoy, Z. Wang, I. Abramovic, P. Vecera, M. Halik, S. Sanvito, G. S. Duesberg, V. Nicolosi, F. Hauke, A. Hirsch, J. N. Coleman and C. Backes, *ACS Nano*, 2015, **9**, 6018–6030.